International Journal of Obesity (2008) 32, 1222–1232
© 2008 Macmillan Publishers Limited All rights reserved 0307-0565/08 $30.00
www.nature.com/ijo

ORIGINAL ARTICLE

Kv1.3 gene-targeted deletion alters longevity and reduces adiposity by increasing locomotion and metabolism in melanocortin-4 receptor-null mice

K Tucker[1,2], JM Overton[2,3] and DA Fadool[1,2,4]

[1]*Department of Biological Science, Florida State University, Tallahassee, FL, USA;* [2]*Program in Neuroscience, Florida State University, Tallahassee, FL, USA;* [3]*Department of Biomedical Sciences, Florida State University, Tallahassee, FL, USA and* [4]*Institute of Molecular Biophysics, Florida State University, Tallahassee, FL, USA*

Objective: Gene-targeted deletion of the voltage-gated potassium channel, Kv1.3, results in 'super-smeller' mice that have altered firing patterns of mitral cells in the olfactory bulb, modified axonal targeting to glomerular synaptic units, and behaviorally have an increased ability to detect and discriminate odors. Moreover, the Kv1.3-null mice weighed less than their wild-type counterparts, have modified ingestive behaviors, and are resistant to fat deposition following a moderately high-fat dietary regime. In this study, we investigate whether or not gene-targeted deletion of Kv1.3 (*Shaker* family member) can abrogate weight gain in a genetic model of obesity, the melanocortin-4 receptor-null mouse (MC4R-null).
Design: Mice with double gene-targeted deletions of Kv1.3 and MC4R were generated by interbreeding Kv1.3 (Kv)- and MC4R-null mouse lines to homozygosity. Developmental weights, nose to anus length, fat pad weight, fasting serum chemistry, oxygen consumption, carbon dioxide respiration, locomotor activity and caloric intake were monitored in control, Kv-null, MC4R-null and Kv/MC4R-null mice. Physiological and metabolic profiles were acquired at postnatal day 60 (P60) in order to explore changes linked to body weight at the reported onset of obesity in the MC4R-null model.
Results: Gene-targeted deletion of Kv1.3 in MC4R-null mice reduces body weight by decreasing fat deposition and subsequent fasting leptin levels, without changing the overall growth, fasting blood glucose or serum insulin. Gene-targeted deletion of Kv1.3 in MC4R-null mice significantly extended lifespan and increased reproductive success. Basal or light-phase mass-specific metabolic rate and locomotor activity were not affected by genetic deletion of Kv1.3 in MC4R-null mice but dark-phase locomotor activity and mass-specific metabolism were significantly increased resulting in increased total energy expenditure.
Conclusions: Gene-targeted deletion of Kv1.3 can reduce adiposity and total body weight in a genetic model of obesity by increasing both locomotor activity and mass-specific metabolism.
International Journal of Obesity (2008) **32,** 1222–1232; doi:10.1038/ijo.2008.77; published online 10 June 2008

Keywords: K channel; energy homeostasis; weight; lifespan

Introduction

The *Shaker* family member, Kv1.3, like other voltage-gated potassium channels, is traditionally considered to contribute to the resting membrane potential, firing frequency and the interspike interval.[1] It is now becoming more evident that voltage-gated ion channels, potassium channels in particular, participate in nontraditional roles including cell proliferation, cell death, cell adhesion and neuronal targeting.[2] The Kv1.3 channel can be modulated in multiple ways: giving rise to complex biophysical control over its many functions. Both receptor and cellular tyrosine kinases, have been shown to acutely suppress Kv1.3 current by direct tyrosine phosphorylation.[3–8] Moreover, tyrosine kinase-mediated suppression of Kv1.3 current can be further modulated by direct protein–protein interactions by adaptor and scaffolding proteins such as postsynaptic density-95 (PSD-95), n-Shc or Grb10.[9,10]

Kv1.3 is involved in a variety of functions and is expressed in both excitable and nonexcitable tissues including, but not limited to, the olfactory bulb,[11] white and brown adipose tissue,[12] skeletal muscle,[12] the hypothalamus,[13] T lymphocytes[14] and their mitochondria,[15] and brain microglia.[16] With this expression pattern in mind, it has not been

Correspondence: Dr DA Fadool, Program in Neuroscience and Molecular Biophysics, Florida State University, 3008 Life Science (KIN), Tallahassee, FL 32306, USA.
E-mail: dfadool@neuro.fsu.edu
Received 19 December 2007; revised 2 May 2008; accepted 3 May 2008; published online 10 June 2008

surprising to find that general gene-targeted deletion of Kv1.3, produces mice with a wide variety of phenotypic outcomes. Kv1.3-null animals have altered axonal targeting of olfactory sensory neurons that synapse at smaller, supernumerary glomeruli in the olfactory bulb.[17] Such modification of olfactory circuitry may underlie the gain of function behaviorally determined in these mice that are 'supersmellers' with increased discrimination of odor molecular features and odor threshold.[18] Furthermore, Kv1.3-null mice weigh 8–12% less than that of their wild-type littermates,[12,18] are resistant to moderately high-fat diet-induced weight gain,[12] are normphagic[12,18] and exhibit increased insulin sensitivity.[19] Acute blockade of Kv1.3 current by margatoxin or genetic deletion of Kv1.3 protein increases peripheral insulin sensitivity by increasing translocation of the glucose transporter 4 (GLUT4) to the membrane in skeletal muscle and white adipose tissue (WAT) in a Ca^{2+} dependent manner by the calcium-sensitive synaptotagmin VII.[19–21]

We now hypothesize that loss of Kv1.3 can abrogate weight gain in a genetic model of obesity that is controlled by the central nervous system (CNS). The melanocortin-4 receptor (MC4R) is a part of the hypothalamic, anorexogenic pathway controlling metabolism and satiety,[22] and brainstem-mediated control of meal size and food preference.[23] Genetic deletion of MC4R results in mice that exhibit severe obesity, hyperphagia, hyperinsulinemia, hypometabolism and increased overall growth.[24,25] We generated mice with a double gene-targeted deletion of Kv1.3 and MC4R by interbreeding Kv1.3-null and MC4R-null mouse lines to double homozygosity. Kv1.3 loss from this genetic model of obesity resulted in a reduction in adiposity and body weight that was not due to overall changes in growth but rather the result of increased locomotor activity and energy expenditure (EE).

Materials and methods

Animal care and generation of double-mutant mouse lines

All mice were housed at the Florida State University vivarium in accordance with the institutional requirements for animal care. Mice were provided food and water *ad libitum* while being maintained on a standard 12/12 h light/dark cycle. Kv1.3-null mice were a generous gift from Drs Leonard Kaczmarek and Richard Flavell (Yale University, New Haven, CT, USA) and were generated as described previously.[12,26] In brief, Kv1.3-null mice were produced by excision of the *Kv1.3* promoter region and one-third of the 5′-coding region as generated in a C57B6/J background.[12,26] The loxTB *Mc4r* mice (MC4R-null) were a generous gift from Dr Joel Elmquist (University of Texas Southwestern Medical Center, Dallas, TX, USA) and were generated as previously described.[27] In brief, the *Mc4r* gene was transcriptionally blocked by insertion of a loxP-flanked transcriptional blocking sequence between the *Mc4r* transcription start sequence and 112 bp upstream of ATG to produce a complete block of *Mc4r* transcription and protein production in a C57B6/J and Sv129 mixed background.[27] Due to the well-known poor reproductive capacity of MC4R(−/−) mice,[28] MC4R(+/−) breeders were maintained and periodically crossed to establish the MC4R-null animals used in the experiments. Also, to increase reproductive success, MC4R(+/−) mice were bred to Kv1.3(−/−) mice to generate an array of useful allelic combinations, which followed traditional patterns of Mendelian inheritance. Double homozygous recessive (Kv/MC4R-null) were backcrossed to wild-type animals to confirm the accuracy of PCR-based genotyping. Standard genotyping was performed by reverse transcriptase–PCR from genomic DNA extracted from tail biopsies using DNeasy Tissue Kit (Qiagen, Valencia, CA, USA). Kv/MC4R-null mice were interbred three generations to establish a working colony. Likewise, double-homozygous dominant (wildtype, WT) were maintained as the experimental wild-type group. Kv1.3-null mice have no difficulty breeding[18] and were therefore used as breeders. A separate group of 20 mice (five of each genotype; WT, Kv-null, MC4R-null and Kv/MC4R-null) were used to assess fecundity within a 10-month window. The ratio of the number of births/number of crosses was calculated for each homozygous breeding pair to determine the pregnancy rate. Thirty-seven mice were monitored for longevity by allowing them to die a natural death.

Indirect calorimetry and behavioral monitoring

Oxygen consumption (VO_2; ml min^{-1}) and carbon dioxide production (VCO_2; ml min^{-1}) of individually housed, post-natal day 60–75 (P60–P75) mice were continuously monitored for 8 days at 23 °C in metabolic isolation chambers as previously described.[29] In brief, mice were placed in shoebox cages ($26 \times 47 \times 13.5$ cm) fitted with near-airtight lids that received fresh air at a rate of 0.5 l min^{-1}. Dry, mixed-cage air was sampled with a 250 ml min^{-1} flow rate and sent to O_2 and CO_2 gas analyzers every 4 min for 30 s followed by VO_2 and VCO_2 determination by open-circuit respirometry according to Bartholomew *et al*.[30] with modifications to isolate successive samples.[29] Due to the established effects of animal size on metabolism and EE and the caveats intrinsic to various approaches to normalize metabolism for body mass,[31] absolute VO_2 (ml min^{-1}), metabolic mass-specific VO_2 (ml min^{-1} per kg of body weight$^{0.75}$),[32] and mass-specific VO_2 (ml min^{-1} per kg of body weight) were calculated. Dark- and light-phase EE were calculated using the Weir equation:[33] $EE = (3.94 \times VO_2) + (1.1 \times VCO_2)$. Total EE (TEE) was calculated as the sum of both the dark- and light-phase EE. All reported mean values were calculated for 12 h of dark and 11 h of light so that daily body weight, caloric intake and water consumption could be measured during the last hour of the light cycle. These manual animal maintenance procedures were purposefully chosen to be performed 1 h before the mice would normally be waking. In

our experience, meal size and activity patterns remain stable due to special housing chambers that isolate animals from external auditory or visual stimulation, see reference Williams *et al*.[34] The extended period of acclimation (3–4 days) prior to physiological measurements additionally minimizes the disturbance of the animals resultant from the daily maintenance, during which, each of the animals is similarly handled. Each cage was positioned on a custom-designed platform resting on a centered fulcrum with stiff strain-gauge load-beam transducers positioned under two adjacent corners to measure animal position and locomotor activity as previously described.[35] Locomotor activity was reported in meters, binned every 30 s, and measured at a 1 mm resolution. Daily caloric intake was calculated by measurement of consumed powdered Purina 5001 rodent chow (3.3 kcal g^{-1}). Photobeam breakage was binned every 30 s with a 50 ms resolution. Drinking behavior was monitored using a lickometer, which recorded licks in 30 s bins.

Fat pad and serum collection

Overnight-fasted P60 mice were weighed and their nose to anus length was recorded. Mice were then anesthetized with 50 mg kg^{-1} of Nembutal followed by decapitation according to Florida State University Laboratory Animal Resources and AVMA-approved methods. Fasting blood glucose levels were determined using an Ascensia Contour Blood Glucose Monitoring System (Bayer Healthcare, Mishawaka, IN, USA) during the collection of trunk blood immediately following decapitation. Collected trunk blood was allowed to coagulate at room temperature (rt) for 10 min, placed on ice for 30 min followed by centrifugation at 750 r.p.m. for 10 min at 4 °C. Serum was collected and stored at −20 °C for later examination with a Mouse Leptin ELISA Kit (Linco Research, St Charles, MO, USA) and an Ultrasensitive Mouse Insulin ELISA Enzyme Immunoassay (Mercodia AB, Uppsala, Sweden) to determine fasting serum levels of leptin and insulin, as per manufacturer's protocols. All visceral fat, including inguinal, retroperitoneal and mesenteric WAT were removed from the abdominal cavity, separated and weighed. Subcutaneous WAT was subsampled by weighing the fat pad on the right side of each animal, from the median line of the abdomen to the spine and the right hip to the first rib. Brown adipose tissue was removed from between the scapulae and weighed.

Data analysis and statistics

Metabolism, EE, locomotor activity, caloric intake and water consumption values were typically 2-day averages after 5–6 days of acclimation of the animal to the metabolic chambers. Statistical significance was determined by one-way analysis of variance (ANOVA) using a Student–Newman–Keuls (SNK) *post hoc* test at the 95% confidence interval.

Results

Kv1.3 removal causes MC4R-null mice to weigh less

To determine if Kv1.3 deletion could prevent weight gain in a genetic model of obesity, Kv/MC4R-null mice were generated by breeding Kv1.3-null[12,26] and MC4R-null[27] mice to homozygosity (see 'Materials and methods'). Targeted deletion of Kv1.3 in MC4R-null mice caused the suppression of late-onset weight gain that typically began around postnatal day 55 (P55) in MC4R-null mice and resulted in a 17.8% decrease in body weight by 9 months of age (Figures 1a and b).

In order to elucidate physiological mechanisms driving reduced weight of Kv/MC4R-null animals, data were sorted by sex to determine the age at which divergence in body weight occurred across the genotypes (Figures 2a and b).

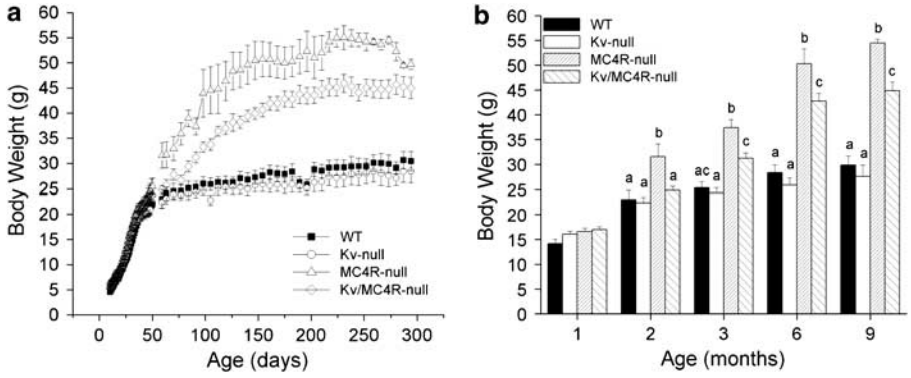

Figure 1 Developmental total body weight is dependent upon genotype. (**a**) Line graph plot of daily (Postnatal day10 (P10) to P50), then weekly, body weight for wild-type mice (WT, $n=6$), Kv1.3 knockout (Kv-null, $n=9$), melanocortin-4 receptor knockout (MC4R-null, $n=6$) and double-knockout mice (Kv/MC4R-null, $n=16$). (**b**) Bar graph representation of total body weight over age in months. Different letters within an age group indicate a significant difference at the 95% percentile as determined by a one-way analysis of variance (ANOVA; treatment = genotype) using a Student–Newman–Keuls (SNK) *post hoc* test. (**a**,**b**) Data represent mean ± standard error of the mean (s.e.m.) in this and all subsequent figures.

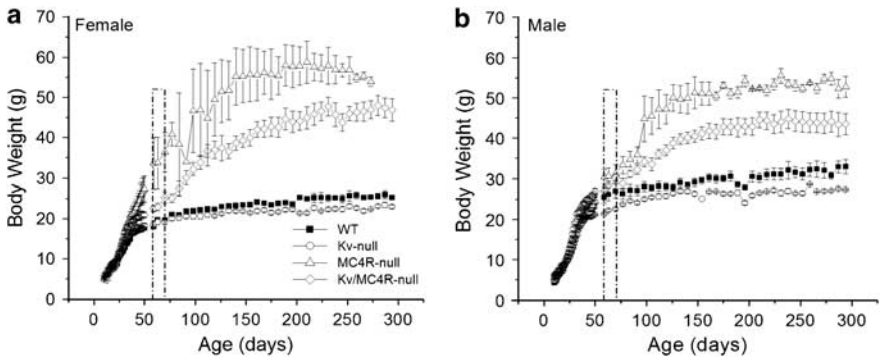

Figure 2 Gender-specific body weight is dependent upon genotype. Graphing and abbreviation as in Figure 1a, but sorted by sex. The dashed box (P60–P75) indicates initial separation in genotype-dependent weight changes and represents the bracketed age group upon which all subsequent experiments were performed (Figures 3–7). Note the higher variability and early weight divergence in female (**a**) when compared to male (**b**) mice. Plotted sample size: (**a**) female (wildtype, WT, $n=2$; Kv-null, $n=3$; melanocortin-4 receptor-null, MC4R-null, $n=2$; Kv/MC4R-null, $n=8$). (**b**) Male (WT, $n=4$; Kv-null, $n=5$; MC4R-null, $n=3$; Kv/MC4R-null, $n=8$).

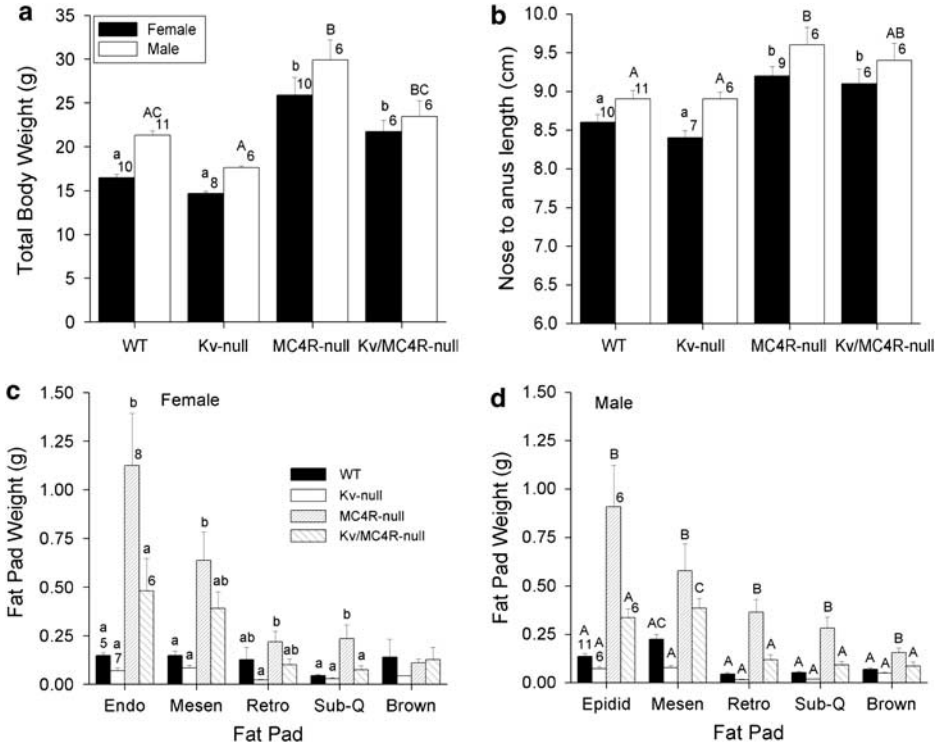

Figure 3 Body weight, growth and adiposity are dependent upon genotype. Histogram plot of (**a**) mean body weight, (**b**) nose to anus length, and (**c**) female, or (**d**) male fat pad deposition sorted by genotype. Abbreviations as in Figure 1. *n*, number of animals; Endo, Endometrial; Epidid, epididimal; Mesen, mesenteric; Retro, retroperitoneal; Sub-Q, subcutaneous; Brown, brown fat. Different lowercase letters denote a significant difference within females and different capital letters indicate a significant difference within males at the 95% percentile as determined by a one-way analysis of variance (ANOVA; treatment = genotype) followed by a Student–Newman–Keuls (SNK) *post hoc* test. Statistics for (**c**) and (**d**) are for within fat pad comparison (treatment = genotype).

Albeit females having slightly greater variability and earlier onset of weight gain, the P60 time point was established as our criteria from which to measure the initiation of changes in correlation to the late-onset weight gain (see dashed lines in Figures 2a and b). Therefore, all subsequent data were collected at P60.

Reduction of body weight in Kv/MC4R-null mice is due to decreased fat deposition

MC4R-null mice have an increased overall growth rate resulting in a greater nose to anus length and increased fat deposition than that of wild-type animals.[24,27] To determine if the reduction in body weight (Figure 3a) was due to a reduced overall growth rate in Kv/MC4R-null animals, nose

to anus lengths were measured as reported in Figure 3b. MC4R-null mouse nose to anus lengths were significantly longer than those of WT and Kv-null mice but were not different from those of Kv/MC4R-null mice. The reduction in body weight of Kv/MC4R-null animals is therefore not likely due to changes in overall growth. Instead, body weight reduction in the Kv/MC4R-null mice appears to be due to a decrease in fat mass deposition. As reported in Figure 3d, male Kv/MC4R-null mice deposit significantly less fat than do male MC4R-null animals in all sampled fat pads including epididymal, mesenteric, retroperitoneal, subcutaneous and brown fat. Female Kv/MC4R-null mice also deposit less fat than do female MC4R-null animals, which reaches statistical significance for endometrial and subcutaneous fat (Figure 3c).

Blood chemistry changes in Kv/MC4R mice

To understand how a Kv1.3-targeted deletion affects resting blood chemistry of MC4R-null mice, trunk blood samples were collected and analyzed from overnight-fasted mice (12 h). As shown in Figure 4a, fasting blood–glucose levels were significantly higher for both male and female MC4R-null and Kv/MC4R-null mice than for those of WT and Kv-null animals. Fasting serum–insulin levels were variable and not significantly different across any genotype (Figure 4b). Fasting serum–leptin demonstrated a highly significant elevation in the MC4R-null mice and was significantly reduced in Kv/MC4R-null animals to levels approximating those measured for WT and Kv-null animals (Figure 4c).

Caloric intake and water consumption

Daily caloric intake in the MC4R-null mice was consistent with our expectations, given that previously published data demonstrating daily caloric changes do not become significant until around 14 weeks of age.[36] Caloric intake was not significantly different across any genotype in comparison to that of WT mice (Figure 5a; not significantly different, ANOVA, SNK). As insignificant differences in caloric intake may become physiologically significant overtime,[25] we also calculated and analyzed a 5-day cumulative food intake (Figure 5b), but similarly, did not find any genotypic changes. There were also no measurable differences in water consumption at this age (Figure 5c). We therefore conclude that the onset of the weight differences at P60, due to gene-targeted deletion of Kv1.3 in MC4R-null mice, is not likely attributed to differences in caloric intake or water consumption.

Dark-phase mass-specific metabolism and locomotor activity are increased in Kv/MC4R-null mice

To ascertain what physiological parameters might be contributing to the reduced adiposity phenotype of Kv/MC4R-null mice, P60–P75 mice were allowed to acclimate to

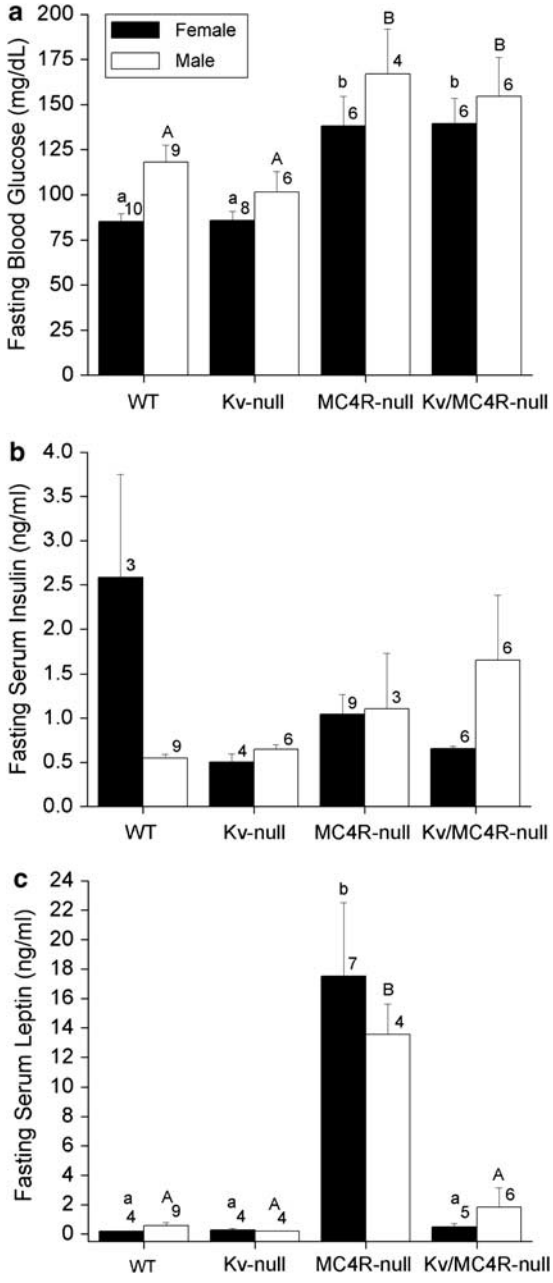

Figure 4 Fasting blood chemistry is dependent upon genotype. Histogram plot of fasting (**a**) blood glucose, (**b**) insulin and (**c**) leptin determined following a 12 h, dark-phase fast. Abbreviations, statistical treatment as per Figure 1.

custom-built metabolic chambers for 4 days followed by 8 baseline days of continuous 12 h of dark-phase and 11 h of light-phase oxygen consumption (VO_2) and locomotor activity monitoring. Figure 6 represents a 2-day average for metabolically active mass-specific metabolism (Figure 6a and b) and locomotor activity (Figure 6c and d). MC4R-null mice displayed a significantly lower dark-phase metabolically

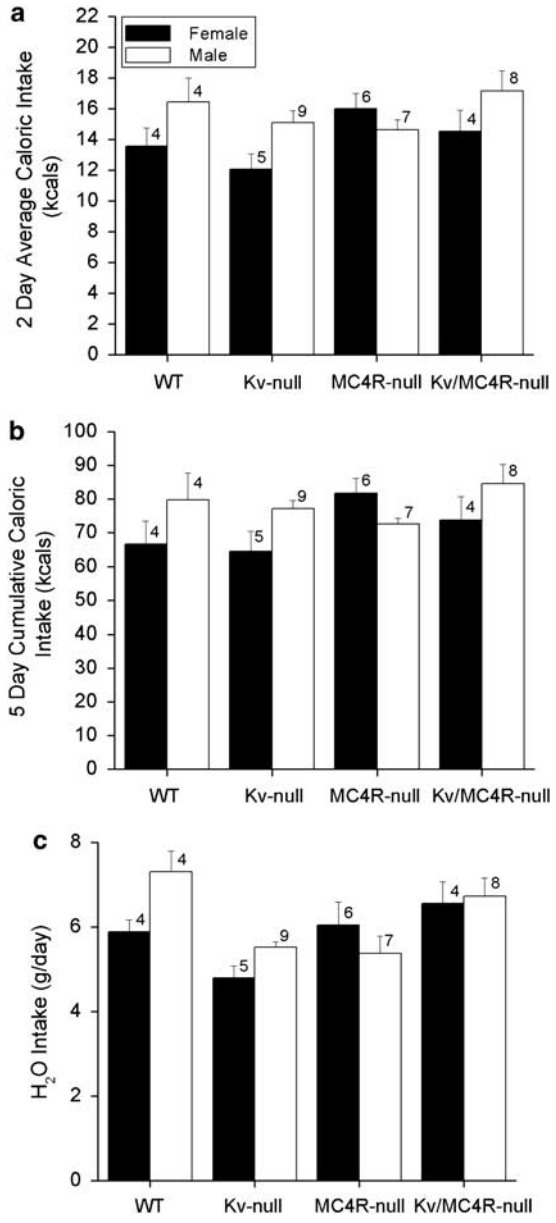

Figure 5 Daily caloric and water intake is not dependent upon genotype. Histogram plot of (**a**) daily caloric intake, (**b**) 5-day cumulative caloric intake and (**c**) water intake. Data represent mean ± s.e.m. of 2-day interval (**a**,**c**) or 5-day cumulative caloric intake (**b**) preceded by a 5-day acclimation period. Abbreviations, statistical treatment as per Figure 1.

active mass-specific metabolic rate (VO_2; $ml\,min^{-1}\,kg^{-0.75}$) when compared to that of WT and Kv-null mice. Gene-targeted deletion of Kv1.3 in MC4R-null mice returned dark-phase metabolically active mass-specific metabolic rate back to that observed for WT animals, completely reversing the low-metabolic phenotype (Figure 6a). The low dark-phase locomotor activity of MC4R-null mice was also reversed by gene-targeted deletion of Kv1.3 in the Kv/MC4R-null mice (Figure 6c). Basal or light-phase metabolically active mass-specific metabolic rate and locomotor activity were not statistically different for any of the genotypes (Figure 6b and d). Due to technical restraints in the measurement and interpretation of open-circuit indirect calorimetry of small animals,[31] we also report uncorrected and weight-corrected oxygen consumption in the light and dark phases as a helpful comparison in Supplementary Figure 1. TEE normalized to body weight (nTEE) was decreased in MC4R-null mice below that of WT and Kv-null animals although gene-targeted deletion of Kv1.3 in MC4R-null mice significantly returned nTEE values to normal levels in females although there was only a trend in males (Figure 7a). When the nTEE is partitioned into energy expended during the dark and light phases, the decrease in expenditure observed in the MC4R-null mice that is corrected by Kv1.3-targeted deletion is statistically preserved in the dark phase but only reaches a trend in the light phase (Figures 7b and c). Therefore, increased dark-phase locomotor activity and concomitant metabolic activity appear to be driving dark-phase EE. Uncorrected energy expenditure values are reported in Supplementary Figure 2.

Kv1.3 *gene-targeted deletion improves longevity and fecundity*
As a result of routine colony maintenance, we observed a differential longevity and pregnancy rate across the generated genotypes, which we then systematically quantified. The mean lifespan of the Kv-null mice significantly increased by 22% over that of WT mice whereby lifespan of the MC4R-null mice, oppositely, was significantly reduced by 36% in comparison to that of WT mice (WT = 778 ± 54 days, Kv-null = 951 ± 40 days, MC4R-null = 497 ± 41 days; Figure 8a). Gene-targeted deletion of Kv1.3 in MC4R-null mice returned the lifespan of these mice to approximately WT levels, 668 ± 84 days (Figure 8a). The survival curve plotting the percentage of mice alive versus age in months demonstrates a similar pattern of increased longevity in the Kv-null background (Figure 8b). Interestingly, the decreased fecundity typically reported for MC4R-null mice[28] was partially rectified in Kv/MC4R-null animals in comparison to the greater than 80% pregnancy rates of either WT or Kv-null mice (Figure 8c).

Discussion

It has previously been shown that Kv1.3 is involved in weight maintenance, diet-induced obesity, peripheral glucose uptake and insulin sensitivity[18–21] We now demonstrate that gene-targeted deletion of Kv1.3 in MC4R-null mice, a genetic model of obesity, reduces adiposity and fasting leptin levels, without changing overall growth, fasting blood–glucose and serum–insulin. Basal or light-phase metabolically active mass-specific metabolic rate and locomotor activity were not affected by genetic deletion of Kv1.3 in MC4R-null mice but dark-phase locomotor activity and

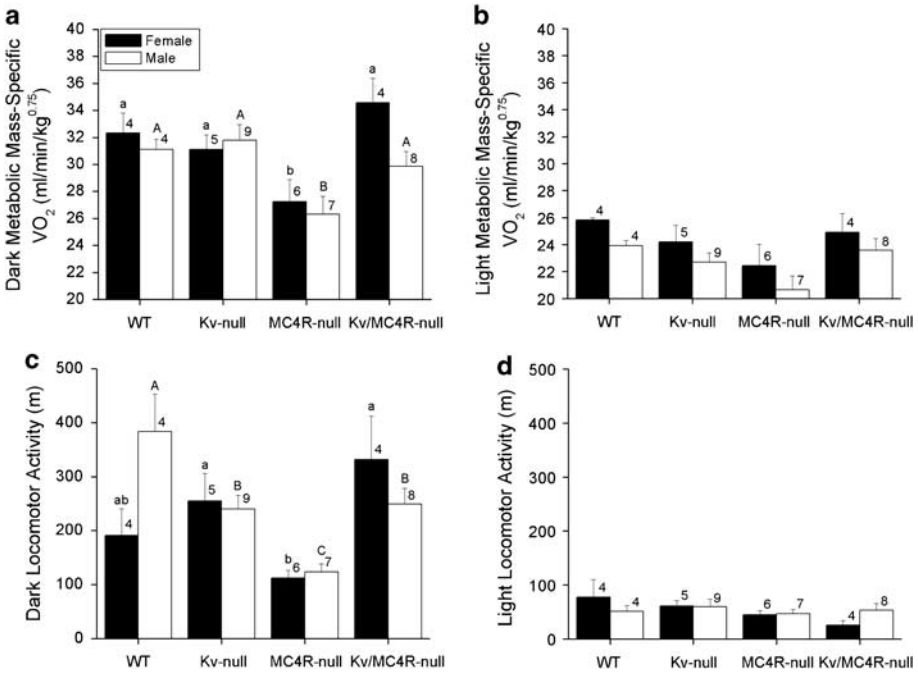

Figure 6 Metabolically active mass-specific metabolic activity and locomotor activity are dependent on genotype. Mice were monitored for 8 days in custom-built metabolic chambers that monitor oxygen consumption (VO_2) and locomotor activity. Histogram plot of (**a**) dark-phase or (**b**) light-phase metabolically active mass-specific VO_2 and dark-phase(**c**) or light-phase (**d**) locomotor activity. Data represent mean ± s.e.m. of 2-day interval preceded by a 5-day acclimation period. Abbreviations, statistical treatment as per Figure 1.

metabolically-active mass-specific metabolism were significantly increased by Kv1.3 deletion resulting in increased mass-specific TEE.

Mutations in the *MC4R* gene are correlated to human obesity in approximately 2–5% of the morbidly obese population.[37] The MC4R-null mouse model of obesity is only one of the several models of genetically-induced obese mouse lines.[38] MC4R-null mice have a first-order mutation in the leptin signaling pathway, and as such, *Kv1.3*-gene deletion likely acts downstream of this pathway. The fact that Kv1.3-null mice are resistant to diet-induced obesity[12] by a hypothesized mechanism that involves increased peripheral GLUT4 translocation in adipose tissue,[19–21] combined with our findings that deletion of the *Kv1.3* gene abrogates genetically-induced obesity that targets a central pathway, may indicate that there are multiple cellular mechanisms for which this Kv channel might regulate energy homeostasis. It might be diagnostic to explore if deletion of Kv1.3 in other obese backgrounds would produce similar decreases in body weight by changes in locomotion or if Kv/MC4R-null animals could curtail weight gain if challenged with a moderately high-fat diet.

MC4R-null mice exhibit a significantly lower metabolic rate than wild-type mice,[27,36] although Kv1.3-null mice have been shown by our group to have no difference in metabolism in animals completely acclimated to the metabolic chambers.[18] Others have reported a significant increase in metabolism in Kv1.3-null mice in short-term (3 h) metabolic studies.[12] Here we confirm previously published data that in long-term metabolic studies, mass-specific metabolism of Kv-null mice is not significantly different from that of WT animals and MC4R-null mice have a significantly lower dark-phase mass-specific metabolic rate than that of both male and female wild-type mice. Kv1.3-targeted deletion in MC4R-null mice returns mass-specific metabolism back to WT levels, reversing the low-metabolic phenotype caused by deletion of MC4R. When one compares the metabolically active mass-specific metabolic rate (Figure 6a) with that of the mass-specific metabolic rate (Supplementary Figure 1c), only the former reaches statistical significance during the dark phase, whereas the latter, reaches only a trend ($P = 0.066$) in males. Therefore, although the mass-specific correction for metabolically active body mass ($kg^{0.75}$) is statistically validated, both forms of normalization demonstrate an identical physiological trend.

Metabolically active TEE was not different between the male MC4R-null and Kv/MC4R-null animals, but it was increased in Kv/MC4R-null females. At the P60 time point of our study, females are more separated in weight and locomotor activity. We did not assess estrous cycle status during our studies of female mice. It is known that estradiol has effects on feeding and locomotor activity in both mice and rats.[39] Examination of food intake and locomotor activity over a 5-day window that would have covered all phases of the estrous cycle, did not demonstrate increased

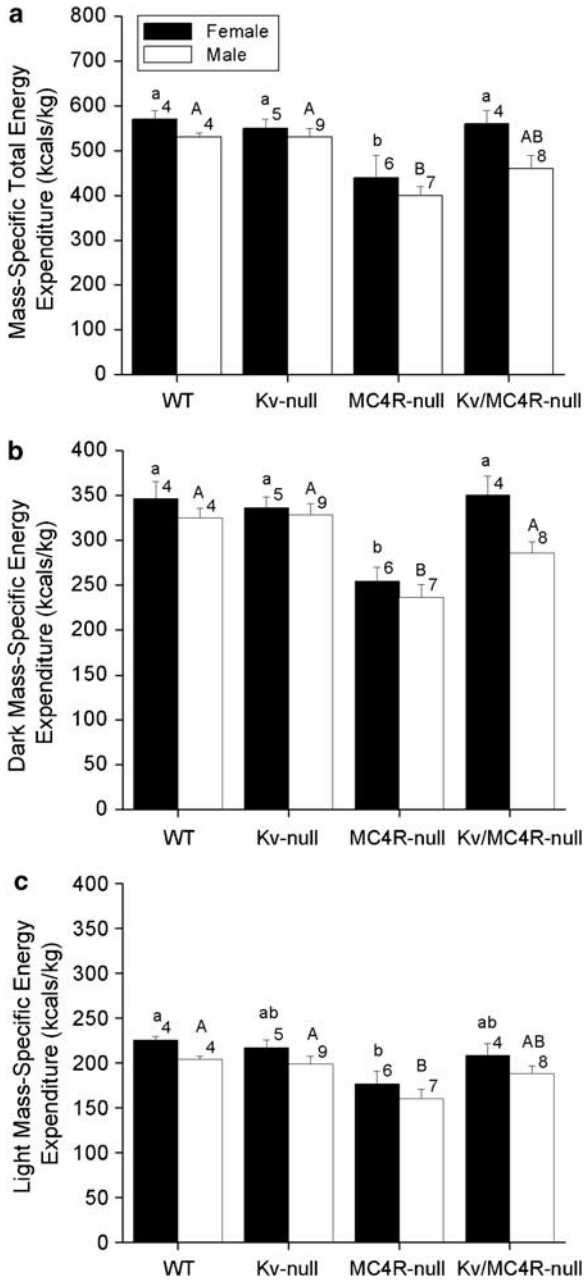

Figure 7 Mass-specific total energy expenditure (TEE) is dependent upon genotype. Histogram plot of the mean (**a**) mass-specific TEE, (**b**) dark-phase and (**c**) light-phase mass-specific energy expenditure sorted by sex and genotype. Data represent mean ± s.e.m. of 2-day interval preceded by a 5-day acclimation period. Abbreviations, statistical treatment as per Figure 1. Mass-specific TEE was calculated as the sum of the 12 h dark-phase and 11 h light-phase energy expenditure, determined by Weir equation, divided by the animal weight (see 'Materials and methods' for details).

variance (data not shown) as one might predict by averaging random stages of a cycle-dependent variable. Moreover, data collected in individual female mice were qualitatively examined but no apparent cyclic changes in activity or food intake were noted. There also seems to be a trend for the male Kv/MC4R-null mice to have a slightly higher caloric intake than that of the MC4R-null mice, possibly leading to a non-statistically significant intermediate EE phenotypic difference in the male mice at P60. Nonetheless, the weight phenotype at month 9 is significantly different for both males and females, suggesting the influence of Kv1.3 on MC4R-null mice is gender independent.

In conjunction with low-metabolic rate, MC4R-null mice have been shown to exhibit decreased locomotor activity or spontaneous physical activity (SPA).[36] Removal of Kv1.3 from MC4R-null mice increased the dark-phase SPA. SPA has been shown in both humans and rodents to contribute to increased TEE by significantly increasing what has been coined NEAT or nonexercise activity thermogenesis or metabolism in both rodents and humans resulting in weight gain resistance.[40] Therefore, it is possible that increased SPA could have increased the dark-phase mass-specific metabolism and mass-specific EE observed in the Kv/MC4R-null mice resulting in a reduced adiposity phenotype. This hypothesis is further strengthened by the fact that no basal or light-phase mass-specific metabolic or locomotor changes were observed, indicating Kv1.3 is not modulating the basal or resting metabolic rate, but only the activity-induced metabolic rate. Likewise, Irani *et al*.[41] were able to show that exercise-induced elevation of locomotor activity decreased MC4R-null mouse body weight by 25% compared to that of sedentary MC4R-null controls. Together, these data suggest that increased SPA seen in the Kv/MC4R-null mice might account for the 18% difference in weight gain between MC4R-null and Kv/MC4R-null mice.

MC4R-null mice and acute block of MC4R by SHU9119 in rats increases meal size and food intake.[23,25,27,36,42] Hyperphagia in MC4R-null mice has been detected as early as P21–P35 by evaluation of cumulative 2-week intake,[25] but daily caloric changes do not become significant until around 14 weeks of age,[36] which is consistent with the results reported here. At 9 weeks of age or approximately P60, the MC4R-null mice did not exhibit statistically significant increases in daily caloric intake over WT or the Kv/MC4R-null mice. This suggests that at P60, caloric intake is not the driving factor for the reduction in total body weight and adiposity in the Kv/MC4R-null mice. In our study, we did not measure cumulative caloric intake to ascertain whether our insignificant differences in calorie intake might cumulate to become physiologically relevant differences over time. Although this is a factor that cannot be eliminated by our current data set, it appears to be less likely given that we have previously measured two of the genotypes (WT versus Kv1.3-null) at 6 months and 1 year of age,[18] where we found that caloric intake did not vary with genotype at older time points.

Both food restriction and adiposity have been demonstrated to affect longevity in rodents.[43–45] All of the animals monitored for lifespan duration in our study were allowed to eat *ad libitum,* therefore, we suggest adiposity had a greater influence in longevity difference over that of food intake. Although our fat-pad analyses were performed at P60, the

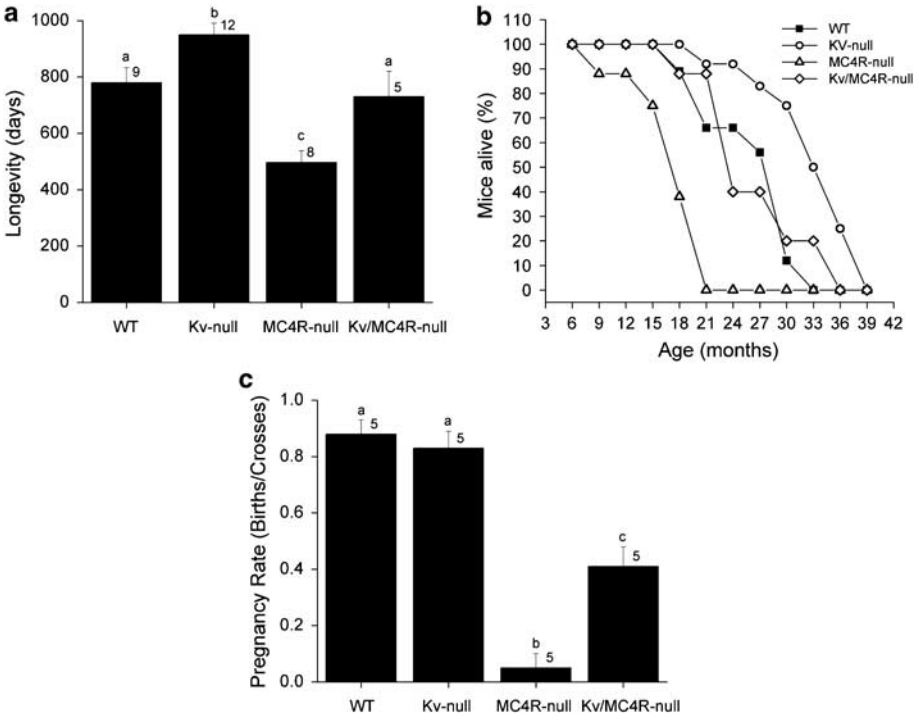

Figure 8 *Kv1.3* gene-targeted deletion improves longevity and fecundity. Histogram plot of the mean (**a**) longevity and (**c**) pregnancy rate calculated as total number of births/total number of crosses for each genotype. Data represent mean ± s.e.m. Abbreviations, statistical treatment as per Figure 1. Survival curve (**b**) depicting the percent survival at various ages. Note the median age of survival for wildtype (WT) is 28 months, Kv-null is 32 months, melanocortin-4 receptor-null mouse (MC4R-null) is 18 months and Kv/MC4R-null mice is 22 months.

further acceleration and then plateau in body weight measured during the first 10 months of age, would suggest that the relative comparison in adiposity across the genotypes would persist throughout the lifespan of the animal. Given the differential in presumed adult fat-pad accumulation, groups of mice with slow metabolism and increased fat-pad accumulation had the shortest lifespan, although mice with increased locomotor activity, metabolism and reduced fat-pad accumulation were correlated with the longest lifespan. A model in which leanness, and not food restriction, was associated with extended longevity was also supported by Bluher *et al.*[46] who demonstrated that fat-specific insulin receptor knockout mice were resistant to age-related obesity and exhibited an increase in lifespan. In tandem with the fact that longevity was improved for the MC4R-null mouse in the *Kv1.3* gene-targeted deletion background, it is interesting that the poor pregnancy rate in these animals was also dramatically improved upon deletion of Kv1.3. Decreased adiposity and increased locomotor activities[41] are two important variables that could contribute to the improved reproductive success of the Kv/MC4R animal.

Brain-derived neurotrophic factor (BDNF) signaling may be involved in an underlying mechanism for our observed reduced adiposity phenotype in the Kv/MC4R-null mice. Certainly BDNF expression is known to increase with exercise[47] and MC4R signaling is known to modulate BDNF expression in the hypothalamus to regulate energy balance.[48,49] From previous investigations, we know that gene-targeted deletion of Kv1.3 results in an increased olfactory bulb expression of the neurotrophin receptor, TrkB.[18] Moreover, activation of the receptor tyrosine kinases, TrkB and insulin receptor kinase, in the olfactory bulb of WT mice results in Kv1.3 current suppression that has been well characterized.[5,7,8] Thus, BDNF signaling in the OB uses Kv1.3 channel protein as a substrate for phosphorylation and subsequent neuromodulation. The channel and neurotrophic pathway reciprocally regulate one another and when the channel is deleted, signaling is uncoupled, and results in such aberrant development such as axonal mistargeting.[17] If we extend this analysis to other CNS regions, where it is known that insulin and BDNF signaling are involved in energy homeostasis (feeding behaviors, locomotor activity and metabolism),[48–55] it could be plausible that Kv-null animals have increased BDNF sensitivity in areas which normally expresses Kv1.3[13] and would be predicted to demonstrate elevated TrkB in Kv-null mice.

More experiments are required to resolve a discrete mechanism that might link loss of Kv1.3 and BDNF activity. Such interactions are likely to be complex, for example, mice heterozygous for BDNF deletion are obese, hyperphagic, hyperinsulinemic, hyperleptinemic and hyperglycemic, but are also hyperactive[56,57] but these mice have reduced BDNF levels through out the entire brain. Other studies, targeting the BDNF signaling cascade in specific regions of the brain

through conditional knockout or nuclei-targeted cannulation studies reveal anatomical separation of the effects of BDNF on feeding, energy metabolism and locomotor activity. The effects of BDNF on feeding but not locomotor activity, have been shown to be mediated by the ventromedial, dorsomedial and paraventricular nuclei (PVN) of the hypothalamus.[53,54,58] The PVN has also been shown to be important for mediating BDNF effects on metabolism but not locomotor activity.[52] BDNF's effects on locomotor activity are localized to the forebrain regions as revealed by forebrain-specific knockouts of *bdnf*[59] and its receptor, *trkB*.[60]

It will be important to investigate the mechanism by which Kv1.3 modulates locomotor activity thereby increasing metabolism and decreasing body weight and adiposity. To do this, it will be necessary to determine which brain regions and cell types express Kv1.3, and in particular, which colocalize the channel and MC4R or TrkB. Acute and chronic blockade of Kv1.3 by siRNA or peptide blockers would be useful to determine if developmental or protein expression changes are responsible for increasing locomotor activity and thereby metabolism in the MC4R-null mouse.

Acknowledgements

We thank Dr Leonard Kaczmarek and Dr Richard Flavell of Yale University School of Medicine, New Haven, CT, for donation of the Kv1.3-null mice and Dr Joel Elmquist of the University of Texas, Southwestern Medical Center, Dallas, TX, for the generous gift of the MC4R-null mice. A special thanks to Thomas Mast, Michelina Messina, Jeffery Godbey, Michael Henderson and Robert Daly for mouse maintenance and technical help. This work was supported by NIH grants DC03387 and T32 DC00044 (NIDCD), the Robinson Foundation (Tallahassee Memorial Hospital) and a CRC planning grant (FSU).

References

1 Bean BP. The action potential in mammalian central neurons. *Nat Rev Neurosci* 2007; **8**: 451–465.
2 Kaczmarek LK. Non-conducting functions of voltage-gated ion channels. *Nat Rev Neurosci* 2006; **7**: 761–771.
3 Bowlby MR, Fadool DA, Holmes TC, Levitan IB. Modulation of the Kv1.3 potassium channel by receptor tyrosine kinases. *J Gen Physiol* 1997; **110**: 601–610.
4 Fadool DA, Holmes TC, Berman K, Dagan D, Levitan IB. Tyrosine phosphorylation modulates current amplitude and kinetics of a neuronal voltage-gated potassium channel. *J Neurophysiol* 1997; **78**: 1563–1573.
5 Fadool DA, Levitan IB. Modulation of olfactory bulb neuron potassium current by tyrosine phosphorylation. *J Neurosci* 1998; **18**: 6126–6137.
6 Cayabyab FS, Khanna R, Jones OT, Schlichter LC. Suppression of the rat microglia Kv1.3 current by src-family tyrosine kinases and oxygen/glucose deprivation. *Eur J Neurosci* 2000; **12**: 1949–1960.
7 Fadool DA, Tucker K, Phillips JJ, Simmen JA. Brain insulin receptor causes activity-dependent current suppression in the olfactory bulb through multiple phosphorylation of Kv1.3. *J Neurophysiol* 2000; **83**: 2332–2348.
8 Tucker K, Fadool DA. Neurotrophin modulation of voltage-gated potassium channels in rat through TrkB receptors is time and sensory experience dependent. *J Physiol* 2002; **542** (Part 2): 413–429.
9 Cook KK, Fadool DA. Two adaptor proteins differentially modulate the phosphorylation and biophysics of Kv1.3 ion channel by SRC kinase. *J Biol Chem* 2002; **277**: 13268–13280.
10 Marks DR, Fadool DA. Post-synaptic density perturbs insulin-induced Kv1.3 channel modulation via a clustering mechanism involving the SH3 domain. *J Neurochem* 2007; **103**: 1608–1627.
11 Kues WA, Wunder F. Heterogeneous expression patterns of mammalian potassium channel genes in developing and adult rat brain. *Eur J Neurosci* 1992; **4**: 1296–1308.
12 Xu J, Koni PA, Wang P, Li G, Kaczmarek L, Wu Y *et al*. The voltage-gated potassium channel Kv1.3 regulates energy homeostasis and body weight. *Hum Mol Genet* 2003; **12**: 551–559.
13 Mourre C, Chernova MN, Martin-Eauclaire MF, Bessone R, Jacquet G, Gola M *et al*. Distribution in rat brain of binding sites of kaliotoxin, a blocker of Kv1.1 and Kv1.3 alpha-subunits. *J Pharmacol Exp Ther* 1999; **291**: 943–952.
14 Decoursey TE, Chandy KG, Gupta S, Cahalan MD. Voltage-dependent ion channels in T-lymphocytes. *J Neuroimmunol* 1985; **10**: 79–95.
15 Szabo I, Bock J, Jekle A, Soddemann M, Adams C, Lang F *et al*. A novel potassium channel in lymphocyte mitochondria. *J Biol Chem* 2005; **280**: 12790–12798.
16 Norenberg W, Gebicke-Haerter PJ, Illes P. Voltage-dependent potassium channels in activated rat microglia. *J Physiol (London)* 1994; **475**: 15–32.
17 Biju KC, Marks DR, Mast TG, Fadool DA. Deletion of voltage-gated channel affects glomerular refinement and odorant receptor expression in the mouse olfactory system. *J Comp Neurol* 2008; **506**: 161–179.
18 Fadool DA, Tucker K, Perkins R, Fasciani G, Thompson RN, Parsons AD *et al*. Kv1.3 channel gene-targeted deletion produces 'Super-Smeller Mice' with altered glomeruli, interacting scaffolding proteins, and biophysics. *Neuron* 2004; **41**: 389–404.
19 Xu J, Wang P, Li Y, Li G, Kaczmarek LK, Wu Y *et al*. The voltage-gated potassium channel Kv1.3 regulates peripheral insulin sensitivity. *Proc Natl Acad Sci USA* 2004; **101**: 3112–3117.
20 Li Y, Wang P, Xu J, Desir GV. Voltage-gated potassium channel Kv1.3 regulates GLUT4 trafficking to the plasma membrane via a Ca2+-dependent mechanism. *Am J Physiol Cell Physiol* 2006; **290**: C345–C351.
21 Li Y, Wang P, Xu J, Gorelick F, Yamazaki H, Andrews N *et al*. Regulation of insulin secretion and GLUT4 trafficking by the calcium sensor synaptotagmin VII. *Biochem Biophys Res Commun* 2007; **362**: 658–664.
22 Butler AA. The melanocortin system and energy balance. *Peptides* 2006; **27**: 281–290.
23 Berthoud HR, Sutton GM, Townsend RL, Patterson LM, Zheng H. Brainstem mechanisms integrating gut-derived satiety signals and descending forebrain information in the control of meal size. *Physiol Behav* 2006; **89**: 517–524.
24 Huszar D, Lynch CA, Fairchild-Huntress V, Dunmore JH, Fang Q, Berkemeier LR *et al*. Targeted disruption of the melanocortin-4 receptor results in obesity in mice. *Cell* 1997; **88**: 131–141.
25 Weide K, Christ N, Moar KM, Arens J, Hinney A, Mercer JG *et al*. Hyperphagia, not hypometabolism, causes early onset obesity in melanocortin-4 receptor knockout mice. *Physiol Genomics* 2003; **13**: 47–56.
26 Koni PA, Khanna R, Chang MC, Tang MD, Kaczmarek LK, Schlichter LC *et al*. Compensatory anion currents in Kv1.3 channel-deficient thymocytes. *J Biol Chem* 2003; **278**: 39443–39451.
27 Balthasar N, Dalgaard LT, Lee CE, Yu J, Funahashi H, Williams T *et al*. Divergence of melanocortin pathways in the control of food intake and energy expenditure. *Cell* 2005; **123**: 493–505.

28 Schioth HB, Watanobe H. Melanocortins and reproduction. *Brain Res Rev* 2002; **38**: 340–350.
29 Rashotte ME, Basco PS, Henderson RP. Daily cycles in body temperature, metabolic rate, and substrate utilization in pigeons: influence of amount and timing of food consumption. *Physiol Behav* 1995; **57**: 731–746.
30 Bartholomew GA, Vleck D, Vleck CM. Instantaneous measurements of oxygen consumption during preflight warm up and postflight cooling in sphinged and saturniid moths. *J Exp Biol* 1981; **90**: 17–32.
31 Arch J, Hislop D, Wang S, Speakman J. Some mathematical and technical issues in the measurement and interpretation of open-circuit indirect calorimetry in small animals. *Int J Obes* 2006; **30**: 1322–1331.
32 Blaxter K. *Energy Metabolism in Animals and Man*. Cambridge University Press: Cambridge, UK, 1989.
33 Weir JB. New methods for calculating metabolic rate with special reference to protein metabolism. *J Physiol (London)* 1949; **109**: 1–9.
34 Williams TD, Chambers JB, Henderson RP, Rashotte ME, Overton JM. Cardiovascular responses to caloric restriction and thermoneutrality in C57BL/6J mice. *Am J Physiol Regul Integr Comp Physiol* 2002; **282**: R1459–R1467.
35 Williams TD, Chambers JB, May OL, Henderson RP, Rashotte ME, Overton JM. Concurrent reductions in blood pressure and metabolic rate during fasting in the unrestrained SHR. *Am J Physiol Regul Integr Comp Physiol* 2000; **278**: R255–R262.
36 Marie L, Miura GI, Marsh DJ, Yagaloff K, Palmiter RD. A metabolic defect promotes obesity in mice lacking melanocortin-4 receptors. *PNAS* 2000; **97**: 12339–12344.
37 Mutch DM, Clement K. Genetics of human obesity. *Best Pract Res Clin Endocrinol Metab* 2006; **20**: 647–664.
38 Carroll L, Voisey J, Van Daal A. Mouse models of obesity. *Clin Dermatol* 2004; **22**: 345–349.
39 Asarian L, Geary N. Modulation of appetite by gonadal steroid hormones. *Philos Trans R Soc Lond B Biol Sci* 2006; **361**: 1251–1263.
40 Novak CM, Levine JA. Central neural and endocrine mechanisms of non-exercise activity thermogenesis and their potential impact on obesity. *J Neuroendocrinol* 2007; **19**: 923–940.
41 Irani BG, Xiang Z, Moore MC, Mandel RJ, Haskell-Luevano C. Voluntary exercise delays monogenetic obesity and overcomes reproductive dysfunction of the melanocortin-4 receptor knockout mouse. *Biochem Biophys Res Commun* 2005; **326**: 638–644.
42 Zheng H, Patterson LM, Phifer CB, Berthoud HR. Brain stem melanocortinergic modulation of meal size and identification of hypothalamic POMC projections. *Am J Physiol Regul Integr Comp Physiol* 2005; **289**: R247–R258.
43 Harrison DE, Archer JR, Astle CM. Effects of food restriction on aging: separation of food intake and adiposity. *Proc Natl Acad Sci USA* 1984; **81**: 1835–1838.
44 Bertrand HA, Lynd FT, Masoro EJ, Yu BP. Changes in adipose mass and cellularity through the adult life of rats fed ad libitum or a life-prolonging restricted diet. *J Gerontol* 1980; **35**: 827–835.
45 McCay CM. Nutritional experiments on longevity. *J Am Geriatr Soc* 1958; **6**: 171–181.
46 Bluher M, Kahn BB, Kahn CR. Extended longevity in mice lacking the insulin receptor in adipose tissue. *Science* 2003; **299**: 572–574.
47 Huang AM, Jen CJ, Chen HF, Yu L, Kuo YM, Chen HI. Compulsive exercise acutely upregulates rat hippocampal brain-derived neurotrophic factor. *J Neural Transm* 2006; **113**: 803–811.
48 Xu B, Goulding EH, Zang K, Cepoi D, Cone RD, Jones KR *et al*. Brain-derived neurotrophic factor regulates energy balance downstream of melanocortin-4 receptor. *Nat Neurosci* 2003; **6**: 736–742.
49 Nicholson JR, Peter JC, Lecourt AC, Barde YA, Hofbauer KG. Melanocortin-4 receptor activation stimulates hypothalamic brain-derived neurotrophic factor release to regulate food intake, body temperature and cardiovascular function. *J Neuroendocrinol* 2007; **19**: 974–982.
50 Ono M, Itakura Y, Nonomura T, Nakagawa T, Nakayama C, Taiji M *et al*. Intermittent administration of brain-derived neurotrophic factor ameliorates glucose metabolism in obese diabetic mice. *Metabolism* 2000; **49**: 129–133.
51 Gray J, Yeo GSH, Cox JJ, Morton J, Adlam AL, Keogh JM *et al*. Hyperphagia, severe obesity, impaired cognitive function, and hyperactivity associated with functional loss of one copy of the brain-derived neurotrophic factor (BDNF) gene. *Diabetes* 2006; **55**: 3366–3371.
52 Wang C, Bomberg E, Billington C, Levine A, Kotz CM. Brain-derived neurotrophic factor in the hypothalamic paraventricular nucleus increases energy expenditure by elevating metabolic rate. *Am J Physiol Regul Integr Comp Physiol* 2007; **293**: R992–1002.
53 Wang C, Bomberg E, Billington C, Levine A, Kotz CM. Brain-derived neurotrophic factor in the hypothalamic paraventricular nucleus reduces energy intake. *Am J Physiol Regul Integr Comp Physiol* 2007; **293**: R1003–R1012.
54 Wang C, Bomberg E, Levine A, Billington C, Kotz CM. Brain-derived neurotrophic factor in the ventromedial nucleus of the hypothalamus reduces energy intake. *Am J Physiol Regul Integr Comp Physiol* 2007; **293**: R1037–R1045.
55 Yamanaka M, Tsuchida A, Nakagawa T, Nonomura T, Ono-Kishino M, Sugaru E *et al*. Brain-derived neurotrophic factor enhances glucose utilization in peripheral tissues of diabetic mice. *Diabetes Obes Metab* 2007; **9**: 59–64.
56 Kernie SG, Liebl DJ, Parada LF. BDNF regulates eating behavior and locomotor activity in mice. *EMBO J* 2000; **19**: 1290–1300.
57 Fox EA, Byerly MS. A mechanism underlying mature-onset obesity: evidence from the hyperphagic phenotype of brain-derived neurotrophic factor mutants. *Am J Physiol Regul Integr Comp Physiol* 2004; **286**: R994–1004.
58 Unger TJ, Calderon GA, Bradley LC, Sena-Esteves M, Rios M. Selective deletion of Bdnf in the ventromedial and dorsomedial hypothalamus of adult mice results in hyperphagic behavior and obesity. *J Neurosci* 2007; **27**: 14265–14274.
59 Monteggia LM, Luikart B, Barrot M, Theobold D, Malkovska I, Nef S *et al*. Brain-derived neurotrophic factor conditional knockouts show gender differences in depression-related behaviors. *Biol Psychiatry* 2007; **61**: 187–197.
60 Zorner B, Wolfer DP, Brandis D, Kretz O, Zacher C, Madani R *et al*. Forebrain-specific trkB-receptor knockout mice: behaviorally more hyperactive than 'depressive'. *Biol Psychiatry* 2003; **54**: 972–982.

Supplementary Information accompanies the paper on International Journal of Obesity website (http://www.nature.com/ijo)